Marine Environmental Research 203 (2025) 106851

Contents lists available at ScienceDirect

Marine Environmental Research

journal homepage: www.elsevier.com/locate/marenvrev

The journey of loggerhead turtles from the Northwest Atlantic to the Mediterranean Sea as recorded by the stable isotope ratios of O, C and N of their bones

Alessandra Cani [a,b,*], Cristina Besén [a,b], Carlos Carreras [b,c], Marta Pascual [b,c], Luis Cardona [a,b]

[a] Departament de Biologia Evolutiva, Ecologia i Ciències Ambientals, Universitat de Barcelona (UB), Av. Diagonal 643, 08028, Barcelona, Spain
[b] Institut de Recerca de la Biodiversitat (IRBio), Universitat de Barcelona (UB), Barcelona, Spain
[c] Departament de Genètica, Microbiologia i Estadística, Universitat de Barcelona (UB), Av. Diagonal 643, 08028, Barcelona, Spain

ARTICLE INFO

Keywords:
Bioapatite
Caretta caretta
Habitat use
Salinity
Skeletochronology

ABSTRACT

Loggerhead turtles, *Caretta caretta*, born on the nesting beaches of the Northwest Atlantic Ocean (US eastern coast) undertake a transoceanic migration immediately after birth, traveling eastward in association with the Gulf Stream and reaching the coasts of Europe and northwestern Africa when two or three years old and 20–30 cm in curve carapace length. Once there, they may remain in the eastern Atlantic or enter the Mediterranean Sea before eventually returning to the western Atlantic several years later. However, the timing of entry into the Mediterranean and the length of the period spent inside are poorly known. To study this, skeletochronology was combined with the analysis of the stable isotope ratios of oxygen ($\delta^{18}O$), carbon ($\delta^{13}C$) and nitrogen ($\delta^{15}N$) in the cortical bone of the humerus of 31 juvenile loggerhead turtles of Northwest Atlantic origin found dead stranded in the Balearic Islands. Incremental bone layers were sampled to assess changes in habitat through the movement across isotopically distinct water masses and the existence of any ontogenetic change in the diet. Although the incremental layers corresponding to the very first years of live were missing in all individuals, the wide range of $\delta^{18}O$ values of the remaining layers suggested that these juveniles moved between water masses differing in salinity, from the eastern Atlantic, the western Mediterranean, and the much saltier eastern Mediterranean, without any consistent temporal pattern. Nevertheless, upon reaching ten years old, loggerhead turtles seem to settle in low salinity areas of the western Mediterranean, such as the Algerian Basin or the Alboran Sea, likely preparing for their return towards their natal beaches in the Northwest Atlantic. Finally, the changes observed in the $\delta^{13}C$ and $\delta^{15}N$ values were small, suggesting only minor ontogenetic changes in their diet throughout the analysed life stages.

1. Introduction

The loggerhead turtle, *Caretta caretta*, is the most common sea turtle species in the Mediterranean Sea (Casale et al., 2018), where individuals from three distinct Regional Management Units can be found: the Mediterranean, the Northwest Atlantic and, to a lesser extent, the Eastern Atlantic (Clusa et al., 2014; Wallace et al., 2023). Loggerhead turtles hatching on the nesting beaches of the Northwest Atlantic disperse along the Gulf Stream (Fig. 1) and reach the coasts of Europe and northwestern Africa when two or three years old and 20–30 cm in curved carapace length (CCL) (Bolten et al., 2003; Hays and Marsh, 1997; Mansfield et al., 2014). Experimental evidence indicates that these juveniles exhibit directional swimming to remain within the North Atlantic Subtropical Gyre (Lohmann et al., 2001, 2012), although some might drift out of the mainstream in association with gyre currents and meso-scale eddies (Mansfield et al., 2014). Eventually, these juvenile loggerhead turtles will reach the Azores, Madeira and the Canary Islands (Mansfield et al., 2009, 2014; Monzón-Argüello et al., 2009) and some will remain several years in the eastern Atlantic [(Varo-Cruz et al., 2016), (Chambault et al., 2019), (Chambault et al., 2021); (Freitas et al.,

* Corresponding author. Departament de Biologia Evolutiva, Ecologia i Ciències Ambientals, Universitat de Barcelona (UB), Av. Diagonal 643, 08028, Barcelona, Spain.
E-mail address: a.cani@ub.edu (A. Cani).

https://doi.org/10.1016/j.marenvres.2024.106851
Received 31 July 2024; Received in revised form 11 November 2024; Accepted 12 November 2024
Available online 17 November 2024
0141-1136/© 2024 The Authors. Published by Elsevier Ltd. This is an open access article under the CC BY-NC-ND license (http://creativecommons.org/licenses/by-nc-nd/4.0/).

2019)] before returning to the Northwest Atlantic when 40–60 cm CCL (Bolten et al., 2003; Mansfield et al., 2009; McClellan and Read, 2007).

During their stay in the eastern Atlantic Ocean, some of the juvenile loggerhead turtles of Northwestern Atlantic origin may enter the Mediterranean Sea (Clusa et al., 2014), where the strong and permanent eastward current at the Strait of Gibraltar (Fig. 1) will prevent them from returning to the East Atlantic until they are approximately 60 cm CCL (Revelles et al., 2007a). However, the entry of juvenile loggerhead turtles in the Mediterranean Sea seems to be a rare event, as only one out of 64 individuals (size range = 23.4–94.6 cm CCL) satellite tracked in the Northeast Atlantic entered the Mediterranean Sea during the tracking period (Canary Islands: n = 24 (Varo-Cruz et al., 2016); Azores: n = 28 (Chambault et al., 2019); Madeira: n = 10 (Freitas et al., 2019); Bay of Biscay: n = 22 (Chambault et al., 2021)). The rarity of such event is, in fact, surprising, considering that juveniles from the Northwest Atlantic population prevail over juveniles of Mediterranean origin in some of the Mediterranean foraging grounds with the highest density of loggerhead turtles in the Mediterranean Sea (Clusa et al., 2014; DiMatteo et al., 2022). Hence, a better understanding on the timing of entry of these juveniles in the Mediterranean Sea is necessary to understand the relevance of this region as a developmental habitat for the Northwestern Atlantic loggerhead turtle population, to assess the significance of the bycatch mortality in the area (de Quevedo et al., 2013) and to predict future changes in the make-up of Mediterranean foraging grounds, especially in a context of environmental changes influencing both the weakening of the Gulf Stream (Piecuch and Beal, 2023) and the Azores current (Frazão et al., 2022) and the inflow across the Strait of Gibraltar (Soto-Navarro et al., 2020).

The use of indirect techniques such as stable isotope analysis has largely increased in the last decades, since they can be informative about a variety of factors such as diet, trophic position, migration patterns and habitat use (Rubenstein and Hobson, 2004). For instance, the oxygen stable isotope ratio ($\delta^{18}O$) in animal tissues reflects that of the water mass where they feed, thus allowing to differentiate between individuals foraging in isotopically distinct areas (Rubenstein and Hobson, 2004; Ben-David and Flaherty, 2012; Newsome et al., 2010; Yoshida and Miyazaki, 1991). In addition, the periosteal bone of the humerus of sea turtles exhibits annual growth bands, also known as incremental layers, which can be used to assess the age of an individual as well as sampled for stable isotope analysis (Ramirez et al., 2015; Snover et al., 2010; Turner Tomaszewicz et al., 2017a). Thus, assessing the $\delta^{18}O$ ratio across the incremental layers of the bone should allow tracking the movement of sea turtles across isotopically distinct water masses.

The Mediterranean Sea has a negative water balance due to an excess of evaporation over precipitation and river runoff, which results in a decrease of sea level, compensated by the entry of Atlantic surface waters through the Strait of Gibraltar (Soto-Navarro et al., 2020; Millot et al., 2005). This process creates a marked and predictable salinity gradient inside the Mediterranean Sea, increasing eastward from the Strait of Gibraltar and reaching the point of maximum salinity at the Levantine Sea (Fig. 1) (Millot et al., 2005; Brasseur et al., 1996). Similarly, regions with an excess of evaporation also present higher $\delta^{18}O$ values in surface waters due to the preferential evaporation of the water molecules carrying the lighter ^{16}O isotope and the resultant concentration of water molecules carrying the heavier ^{18}O isotope (Sharp, 2017), which creates a positive and linear correlation between salinity and $\delta^{18}O$ values (Gat, 1996; Conroy et al., 2014). Therefore, the $\delta^{18}O$ values of Mediterranean surface waters reflect the same gradual increase as those of salinity from the Strait of Gibraltar to the eastern basin (Fig. 1) (LeGrande and Schmidt, 2006) and this relationship facilitates the use of the $\delta^{18}O$ as a habitat tracer to analyse animal movement, distribution and habitat use within the Mediterranean Sea (Belem et al., 2019; Cani et al., 2024).

Additionally, the carbon ($\delta^{13}C$) and nitrogen ($\delta^{15}N$) stable isotope ratios have been widely used to study the trophic ecology of marine animals (Newsome et al., 2010; Ramos and González-Solís, 2012). The former indicates the primary source of carbon in the diet, with generally higher $\delta^{13}C$ values observed in benthic and coastal species and lower values found in pelagic and offshore consumers, whereas the latter increases consistently along the food web due to the trophic enrichment and thus allows for the assessment of trophic position of species or individuals (Rubenstein and Hobson, 2004; Newsome et al., 2010). Hence,

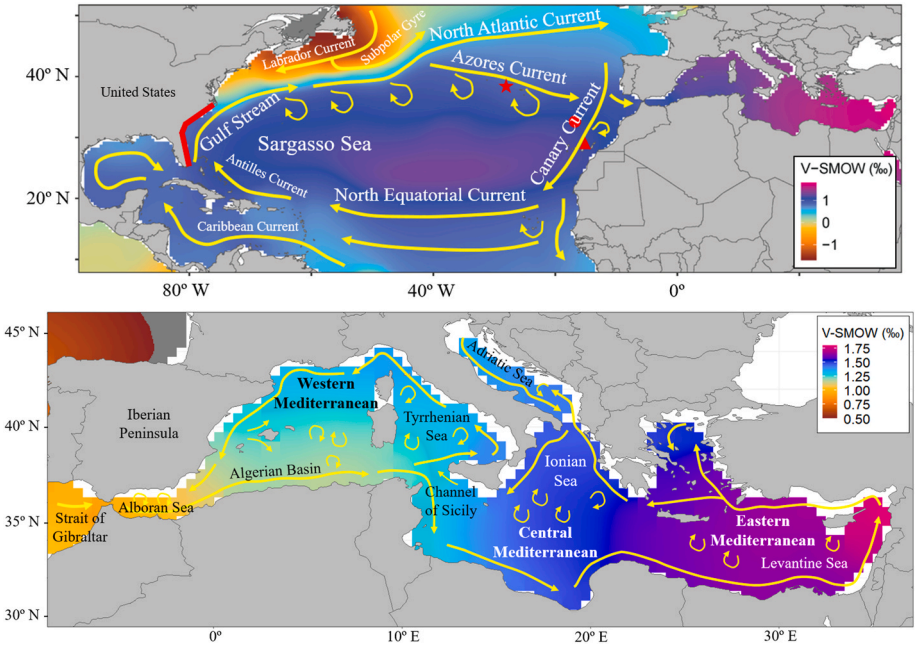

Fig. 1. Main currents of the North Atlantic Ocean (above) and the Mediterranean Sea (below); background colours represent the sea surface mean $\delta^{18}O$ values as indicated by the corresponding scale. Yellow arrows show the general path of the local currents, including gyres and meso-scale eddies. Red features in the top panel show, from left to right, the position of the nesting beaches of the Northwestern Atlantic (thick line), the Azores (star), Madeira (circle) and the Canary Islands (triangle). Sea surface $\delta^{18}O$ values were obtained from LeGrande and Schmidt (LeGrande and Schmidt, 2006) (data available at: https://data.giss.nasa.gov/o18data/grid.html).

the $\delta^{13}C$ and $\delta^{15}N$ values can be potentially used to identify changes in the diet and trophic position of loggerhead turtles (Cardona et al., 2014).

The present study uses the $\delta^{18}O$, $\delta^{13}C$ and $\delta^{15}N$ values of incremental layers in the humerus of loggerhead turtles, previously confirmed to be of Northwestern Atlantic origin through genetic analysis (Clusa et al., 2014), found dead stranded in the Balearic Islands to assess the timing of entry into the Mediterranean Sea, analyse their movements across isotopically distinct water masses and identify any ontogenetic changes in the diet during their stay in developmental habitats.

2. Methods

2.1. Study area

The Gulf Stream is one of the main currents of the North Atlantic Ocean, playing an important role on water circulation and climate for the northern hemisphere (Palter, 2015). It flows northwards along the coast of Florida until around 35° N, where it separates from the continental slope and moves eastward towards the Azores to form the North Atlantic Current and the Azores Current (Fig. 1) (Fofonoff et al., 1981; Schmitz et al., 1993). The latter then turns into the Canary Current, which flows southward along the western coast of South Africa and then returns to the western North Atlantic as the North Equatorial Current (Fig. 1). However, part of the Azores Current reaches the Strait of Gibraltar and enters the Mediterranean Sea as the Algerian Current, circulating in a counter-clockwise direction through the entire basin and getting continuously transformed into a denser water mass that will eventually sink and outflow back into the eastern North Atlantic (Fig. 1) (Millot et al., 2005; Fofonoff et al., 1981; Schmitz et al., 1993).

The Mediterranean Sea is a semi-enclosed system divided into three main basins according to their location and properties: western, central and eastern basins (Fig. 1) (Millot et al., 2005). The western basin is characterized by a constant inflow of fresher Atlantic surface waters from the Strait of Gibraltar in the southwest, passing through the Alboran Sea and the Algerian Basin (Fig. 1). Part of these Atlantic waters stay within the boundaries of the western basin, moving northwards through the Tyrrhenian Sea, reaching the coasts of the Iberian Peninsula from the north and closing the western Mediterranean gyre at the Alboran Sea (Fig. 1) (Millot et al., 2005). At the same time, another part of these waters continues alongslope the Algerian Basin towards the central basin through the Strait of Sicily, eventually reaching the Levantine Sea and becoming part of the eastern Mediterranean gyre (Fig. 1). As it circulates, the higher evaporation rate in the eastern Mediterranean increases the salinity and hence the density of this water mass, causing its sinking at specific zones in the northern parts of each basin (Millot et al., 2005).

Fig. 1 shows an isoscape of the study area for the $\delta^{18}O$ values of the upper 5 m of seawater, based on the estimations made by LeGrande and Smith (LeGrande and Schmidt, 2006), which combined direct observations with regional estimates of the $\delta^{18}O$ to salinity relationship.

2.2. Sampling

Humeri of 31 loggerhead turtles stranded or incidentally caught off the Balearic Islands between 2002 and 2007, and previously confirmed to be of Northwestern Atlantic origin through individual assignments using genetic analysis (Clusa et al., 2014), were selected from the tissue bank of the University of Barcelona. For all individuals, the curved carapace length (CCL) notch-to-notch was measured when necropsied for samples. More recent samples were not included in the analysis because the recent colonization of the western Mediterranean since 2010 by nesting females of both Mediterranean and Northwest Atlantic origin (Cardona et al., 2024; Carreras et al., 2018; Luna-Ortiz et al., 2024) have dampened the resolution of mitochondrial haplotypes and microsatellites for individual assignation to regional management units.

Two contiguous cross sections made in between the deltopectoral crest and the narrowest part of the right humerus of each individual were used (Goshe et al., 2020; Zug et al., 1986). The first cross section, of approximately 5 mm thick along the longitudinal axis of the bone, was decalcified with 5 % nitric acid for 3–4 days (Bjorndal et al., 2000) and subsequently dehydrated and fixed in paraffin wax according to the protocol described by Durfort (1987) as follows: 12 h immersion in 70 % ethanol, 12 h in 90 % ethanol, 12 h in 100 % ethanol, 5 h in 100 % chloroform, 5 h in chloroform saturated with paraffin and, lastly, 5 h in the oven while submerged in paraffin. The decalcified and dehydrated samples were then embedded in paraffin wax using a paraffin dispenser and left at room temperature to solidify. Histological sections of 10–20 μm thick were obtained using a Rotary Microtome and placed on a glass slide for the posterior Hematoxylin-Eosin staining (Cardiff et al., 2014). Each stained section was observed using an Olympus SZX10 Stereo Microscope and analysed with the cellSens Imaging Software to identify the incremental layers in the cortical bone. At least two stained sections were used per sample to confirm the continuity of the observed incremental layers, which were counted twice by two independent readers each time (LC, AC or CB). Counts matched in 25 samples and for the five samples that differed the last count performed was used.

The second cross section, of approximately 3 cm thick along the longitudinal axis of the humerus, was affixed to a surface and used to obtain the powdered bone samples for the stable isotope analysis using a hand drill with a fine diamond tip (Fig. 2, a), obtaining between 2.0 and 3.0 mg of powdered bone for each sampled layer. Two (n = 17) or three (n = 14) layers between 2 and 3 mm deep were sampled from each humerus (Fig. 2, a), with a total of 76 samples. The resulting bone powder was homogenized and weighted as explained in subsection 2.3.

The cortical bone of a turtle's humerus is formed by periosteal deposition, and the innermost incremental layers, corresponding to the earlier years of life and remaining closer to the medullar bone, often suffer an endosteal resorption (Zug et al., 1986). For this reason, the estimation of the age of each individual resulted from the sum of the total number of incremental layers observed, and the estimated number of reabsorbed layers (Suppl. Table 1), which was calculated using the regression equation derived from the correction-factor protocol described by Parham and Zug (1997). Briefly, for each humerus, the diameter of the resorption core was measured, which included the medullar cavity and any endosteal bone deposited in the area of resorption where incremental layers were lost (Zug et al., 1986; Piovano et al., 2011). The correction-factor protocol (Parham and Zug, 1997) was chosen since it was the method that showed the least variation and that adjusted best to the observed pattern of bone growth in loggerhead turtles. Moreover, it provides a direct estimation of the relationship between the resorption core radius and the number of lost layers based on an empirically derived relationship. This regression equation was derived from a subsample of small turtles with CCL <70 cm and a few larger individuals added to establish a growth trajectory; thus, it accounts for the different distribution of the incremental layers in the cortical bone as the individual grows, since the outermost layers (those corresponding to the last years of the turtle's life) tend to be closer together than the innermost layers (those corresponding to the earlier years of the turtle's life). The regression equation used for this purpose was as follows:

$$\#\ Lost\ layers = (r_{rc} - 0.407) / 0.75 \quad (1)$$

where r_{rc} is the radius of the resorption core, obtained by dividing the measured diameter by two (Parham and Zug, 1997).

The ages covered by each sampled bone layer were determined by cross-referencing the position of each sample (i.e., where the bone powder was obtained for stable isotope analysis) with that of the counted incremental layers after the staining procedure, based on the measurements between sampled layers and using the outermost part of the bone and the resorption core as references (Fig. 2, b). When more than one year was covered by the same sample, the highest age of the

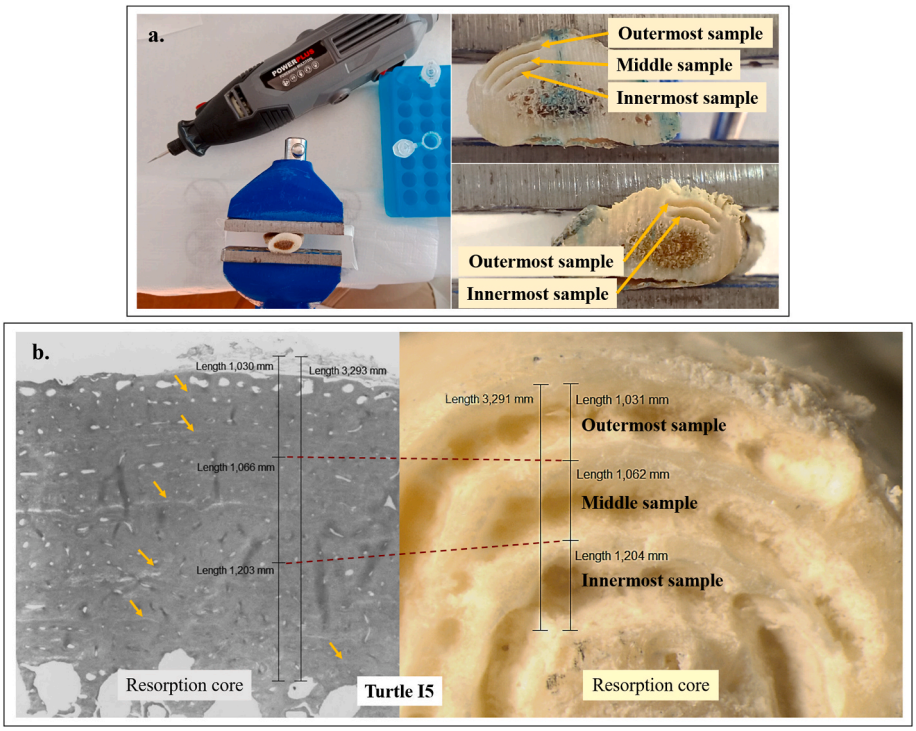

Fig. 2. a) Bone sampling of three (outermost, middle and innermost) or two (outermost and innermost) layers from the second cross-section of the humerus. **b)** Example of the method for cross-referencing the position of each observed incremental layer (yellow arrows on the left) to that of the contiguous section of the same bone that was sampled for stable isotope analysis (the colour of this image was edited to better show the incremental layers).

Table 1
Oxygen stable isotope ratio ($\delta^{18}O$), estimated age and years covered for each sampled incremental layer for all the considered individuals.

Turtle			Cortical bone samples								
			Innermost layer			Middle layer			Outermost layer		
ID	CCL (cm)	Age	$\delta^{18}O_{SMOW}$ (‰)	Age	Years covered	$\delta^{18}O_{SMOW}$ (‰)	Age	Years covered	$\delta^{18}O_{SMOW}$ (‰)	Age	Years covered
A4	28.00	4	32.75	3	2	–	–	–	33.00	4	1
M12	36.00	5	34.47	4	2	–	–	–	34.38	5	1
A10	41.83	6	33.50	4	2	–	–	–	33.20	6	2
A36	43.00	6	32.09	4	2	32.01	7	2	32.78	6	2
M11	45.94	6	33.66	4	1	33.19	5	1	32.78	6	1
M15	47.50	6	33.38	4	2	–	–	–	33.52	6	2
M7	47.62	8	32.50	6	3	–	–	–	33.19	8	2
A8	48.50	7	33.48	5	2	–	–	–	33.73	7	2
A20	48.50	[a]8	33.84	–	–	–	–	–	33.18	–	–
I4	48.67	9	32.87	5	2	33.53	7	2	32.79	9	2
M19	50.00	7	32.75	4	1	33.43	5	1	32.92	7	2
M14	52.00	7	32.20	5	3	–	–	–	33.04	7	2
A7	52.65	7	33.21	5	2	–	–	–	33.01	7	2
A1	53.00	7	32.86	4	1	32.39	6	2	32.79	7	1
A19	53.46	7	31.88	4	2	31.90	6	2	32.87	7	1
A14	54.00	9	31.86	6	4	–	–	–	32.77	9	3
A23	54.00	8	32.03	5	2	32.38	7	2	32.34	8	1
A21	54.22	6	33.63	5	2	–	–	–	33.74	6	1
A35	57.40	10	32.58	7	4	–	–	–	32.29	10	3
A13	58.50	10	32.62	6	3	32.02	8	2	33.83	10	2
A6	59.00	7	33.79	5	1	34.11	6	1	34.13	7	1
I5	59.00	9	33.45	5	2	32.66	7	2	33.44	10	3
A32	61.50	8	33.43	6	3	–	–	–	33.36	8	2
A29	62.00	8	33.76	6	2	–	–	–	34.31	8	2
A18	66.80	9	33.30	5	1	33.67	7	2	33.28	9	2
A26	67.00	9	31.31	7	3	–	–	–	31.63	9	2
A15	69.00	10	32.78	6	2	31.02	8	2	32.59	10	2
A39	70.00	13	31.89	9	3	–	–	–	32.05	13	4
A22	70.85	14	30.87	10	4	–	–	–	32.19	14	4
M17	76.00	15	31.98	9	3	31.86	12	3	31.99	15	3
A28	80.64	14	32.47	10	3	31.73	12	2	33.21	14	2

[a] assumed on the basis of the age of turtles of similar CCL.

estimated range was assigned (Table 1). Finally, it was not possible to determine the age of turtle A20, since the poor condition of the bone hindered the observation and counting of the incremental layers; thus, this individual was not considered for the age-related analysis. However, for discussion purposes, we assumed that turtle A20 was approximately eight years old, based on the mean of the ages estimated for turtles of similar CCL (A8 and I4; Table 1).

2.3. Stable isotope analysis

2.3.1. Oxygen stable isotopes

Between 1.5 and 2.0 mg of each of the homogenized bone samples were soaked in 30% hydrogen peroxide (H_2O_2) for 48 h to remove any organic compounds, and then rinsed repeatedly with deionized (Milli-Q) water and treated with 1 M of calcium acetate–acetic acid buffer for another 24 h to remove any diagenetic carbonate. Finally, they were carefully rinsed again with Milli-Q water and dried for 24 h and left to dry in an oven at 50 °C for another 24 h (Koch et al., 1997).

Approximately 1.0 mg of each treated bone sample was weighed and dissolved in 100 % phosphoric acid at 70 °C with concurrent cryogenic trapping of CO_2 and H_2O. The CO_2 was then admitted to a Finnigan MAT 252 Isotope Ratio Mass Spectrometer (IRMS) with Kiel III Carbonate Analysis Device (Thermo Fisher Scientific) to obtain the isotopic ratio. Two internal isotopic reference materials, RC-1 and CECC with $\delta^{18}O$ values relative to the Vienna Pee Dee Belemnite (V-PDB) calcium carbonate of −2.08 ‰ and −17.56 ‰, respectively, were employed once every five analysed samples in order to recalibrate the system and compensate for any measurement drift over time. Internationally certified isotope secondary standards distributed by the International Atomic Energy Agency (IAEA) of known $^{18}O/^{16}O$ ratios were then used to confirm the results. These consisted of the NBS-19, NBS-18 and IAEA 603 calcite standard, with $\delta^{18}O$ values of −2.20 ‰, −23.2 ‰ and −2.37 ‰, respectively, relative to V-PDB. The analytical precision of $\delta^{18}O$ tested by replicate analyses was ±0.04 ‰ (standard deviation). Because $\delta^{18}O$ values in animal studies are more commonly presented relative to the Vienna Standard Mean Oceanic Water (V-SMOW) index, $\delta^{18}O$ values were converted from V-PDB to V-SMOW according to the following equation (Cardona et al., 2014):

$$\delta^{18}O_{(SMOW)} = \left[\delta^{18}O_{(PDB)} \text{ x } 1.03086\right] + 30.86 \quad (2)$$

2.3.2. Carbon and nitrogen stable isotopes

Approximately 1.0 mg of each of the homogenized bone samples were weighted and encapsulated in tin capsules (3.3 × 5 mm) for $\delta^{13}C$ and $\delta^{15}N$ determination. No pre-treatment was applied since the lipid content of the cortical bone of sea turtles is low (Turner Tomaszewicz et al., 2015). Samples were combusted at 900 °C using a Delta V Advantage isotope ratio mass spectrometer with a Flash IRMS elemental analyzer and CONFLO IV interface (Thermo Fisher Scientific). Isotopic reference materials of known $^{13}C/^{12}C$ ratios were: IAEA CH7 ($\delta^{13}C$ = −32.15 ‰), UCGEMA SC ($\delta^{13}C$ = −13.21 ‰), UCGEMA CH ($\delta^{13}C$ = −22.08 ‰), fructose ($\delta^{13}C$ = −10.80 ‰), and USGS 62 ($\delta^{13}C$ = −14.79 ‰). Isotopic reference materials of known $^{15}N/^{14}N$ ratios were: UCGEMA CH ($\delta^{15}N$ = −4.81 ‰), IAEA N1 ($\delta^{15}N$ = 0.40 ‰), UCGEMA P ($\delta^{15}N$ = 7.60 ‰), UCGEMA SC ($\delta^{15}N$ = 12.40 ‰), IAEA 600 ($\delta^{15}N$ = 1.00 ‰), USGS 62 ($\delta^{15}N$ = 20.17). All these isotopic reference materials were used at the beginning and at the end of the whole run and different combinations of two of them were used to recalibrate the system once every 16 samples, in order to compensate for any measurement drift over time. Analytical precision for repeated measurements of the reference material, run in parallel with the bone samples, was 0.4 ‰ for $\delta^{13}C$ and 0.3 ‰ for $\delta^{15}N$.

2.4. Data analysis

All statistical analyses and plots were carried out using R Statistical Software v 4.1.2 (R Core Team, 2021). Normality was assessed through the Lilliefors test and homoscedasticity by means of the Levene test. All data was confirmed to follow a normal distribution, except age ($D = 0.186$, $p < 0.001$), thus, parametric and non-parametric tests were applied accordingly. The relationship between the $\delta^{18}O$, $\delta^{13}C$ and $\delta^{15}N$ values of each sampled incremental layer and their corresponding estimated age was determined with Kendall's rank correlation (tau) and an adjusted Generalized Additive Model (GAM) with the isotopic ratios as the response variable, the age as the explanatory variable to which a smoothing spline was included in order to capture non-linear relationships, and the individual's ID as a random factor.

Two-dimensional plots were built using the package "SIBER" (Stable Isotope Bayesian Ellipses) (Jackson et al., 2011) to estimate the isotopic niche width and overlaps between the different ages for the $\delta^{13}C$ and $\delta^{15}N$ isotopic space (isospace). Most age classes were analysed independently, but animals of 3 and 4 years old and those ranging 12–15 years old were pooled together, respectively, because sample size was too small to calculate the standard ellipses using SIBER (Jackson et al., 2011). The isotopic niche width was estimated as the standard ellipse area of each age class, corrected for small sample size (SEAc) (Jackson et al., 2011). This approach was preferred over the Bayesian estimate of the standard ellipse because allows plotting the isotopic niche of each species within the isospace and to calculate the overlap among species. Moreover, the relationship between the SEAc in the $\delta^{13}C$-$\delta^{15}N$ isospace and age was further analysed with Kendall's rank correlation (tau) and an adjusted Generalized Additive Model (GAM), with the SEAc as the response variable and the age as the explanatory variable.

In addition, the magnitude of the difference between the $\delta^{18}O$, $\delta^{13}C$ and $\delta^{15}N$ values of the outermost, the middle (when applicable), and the innermost incremental layer per individual was compared with the magnitude of the difference of known environmental values of the North Atlantic Ocean and the Mediterranean Sea, to analyse changes in the habitat use over time (Fig. 4). For this, the differences in $\delta^{18}O$ values between incremental layers of each turtle were compared to the isoscape presented in Fig. 1, based on the estimations made by LeGrande & Smith (LeGrande and Schmidt, 2006) and available at the Global Seawater Oxygen Isotope Database (https://data.giss.nasa.gov/o18data/). Considering the endosteal resorption of the innermost incremental layers explained above, and thus the loss of the information about the first years of life corresponding to the time spent in the Gulf Stream, only the surface waters between Azores and the European/Northeast African coast were considered. In this case, the magnitude of the difference between the lowest $\delta^{18}O$ values found at the nearby North Atlantic waters (0.80 ‰) and the highest values found at the Easternmost part of the Mediterranean (1.80 ‰) is ±1.00 ‰. Furthermore, a mean increase of 0.25 ‰ was found between Mediterranean regions (i.e., Strait of Gibraltar and Alboran Sea, western Mediterranean basin, central Mediterranean basin, and eastern Mediterranean basin). Hence, only those individuals with a difference larger than ±0.25 ‰ between incremental layers were considered to have moved between regions, whereas those with a difference larger than ±1.00 ‰ were likely to move from one side to the other of the Mediterranean Sea. The direction of these migrations for each individual was determined by the sign of the value (e.g., positive differences indicate movement towards waters with higher $\delta^{18}O$ values, and vice versa).

Regarding the $\delta^{13}C$ values, the difference between layers was compared to the difference between the mean values of the oceanic particulate organic matter (−23.1 ‰) and the neritic seagrass *Posidonia oceanica* (−13.0 ‰) off the Balearic Islands, according to Cardona et al. (2007), which is ±10.1 ‰. The direction of the movement was also determined by the sign of the value (e.g., positive differences indicate movements towards oceanic waters with lower $\delta^{13}C$ values, and vice versa). Finally, the $\delta^{15}N$ values were compared to ±3.4 ‰, the mean trophic fractionation in aquatic food webs according to Post (2002).

Finally, Straight Carapace Length (SCL) values reported in the literature were converted to Curved Carapace Length (CCL) using the

following unpublished equation, derived by the authors for loggerhead turtles found in the Mediterranean Sea:

$$CCL = [SCL + 0.129] / 0.926 \quad (3)$$

3. Results

The curved carapace length (CCL) of the 31 analysed loggerhead turtles ranged from 28.0 to 80.6 cm, with a mean value of 55.4 ± 11.5 cm CCL (Table 1). The age when stranded was estimated for 30 turtles, as it was not possible for individual A20, and ranged from 4 to 15 years old with a mean of 8.3 ± 2.7 years old (Table 1). Bone sampling for the stable isotope analysis of these 30 individuals yielded 74 samples, with sample ages ranging from 3 to 15 years old (7.1 ± 2.6 years old; Table 1). In addition, each sampled layer covered between one and four years of a turtle's life, because of large differences in layer thickness. In most cases (54.1 %), each layer corresponded to two consecutive years, others (21.6 %) to only one year, and the rest corresponded to three and four years (17.6 % and 6.8 %, respectively).

When pooled together, the $\delta^{18}O$ values obtained for the incremental layers of the humerus of the analysed individuals ranged from 30.9 to 34.5 ‰ (32.9 ± 0.8 ‰; Table 1; Fig. 3, a). Therefore, the maximum difference between the bone $\delta^{18}O$ values was 3.6 ‰, which is considerably larger than the estimated difference between the $\delta^{18}O$ ratio of surface waters for the study area (1.00 ‰; see Methods), hence suggesting the use of isotopically different water masses between individuals. Furthermore, the $\delta^{18}O$ values of the incremental layers corresponding to less than 10 years old, which included 29 turtles, were considerably scattered, whereas those of 10 years and older, which included 10 turtles, were clustered around a lower mean $\delta^{18}O$ value (Fig. 3, a). The age of the incremental layers and their respective $\delta^{18}O$ values were negatively correlated (Kendall's rank correlation: $\tau = -0.24$, $z = -2.83$, $p = 0.004$) and the adjusted GAM, which accounted for 80.3 % of the variability in the data, suggested a predominantly linear relationship between the two variables (GAM model: R^2 (adj) = 0.67, GCV = 0.36, Scale est. = 0.21; Fig. 3, a). Furthermore, 24 out of the 31 considered turtles showed differences equal or larger than ±0.25 ‰ between at least two of the analysed incremental layers (Table 1; Suppl. Table 2), which is the estimated difference in the $\delta^{18}O$ ratio of surface waters between Mediterranean basins (see Methods; Fig. 4) and thus indicates the use of water masses with distinct $\delta^{18}O$ values throughout the analysed periods.

On the other hand, when analysing individual movement patterns, four different scenarios appeared. First, 17 turtles had the highest $\delta^{18}O$ value in their innermost incremental layer compared to the middle and/or outermost ones (Table 1; Suppl. Table 2; Suppl. Fig. 1), suggesting a continuous movement from ^{18}O-enriched to ^{18}O-depleted waters. However, four of them (A1, I5, A15, A28) also showed a decrease in the $\delta^{18}O$ value of their middle layer compared to the other two, seemingly going from ^{18}O-enriched to ^{18}O-depleted and back to ^{18}O-enriched waters. On the contrary, a second group of four turtles (A10, M11, A20, A35), three of which were estimated to be six and seven years old, showed the highest $\delta^{18}O$ value in their outermost incremental layer compared to the middle and/or innermost ones (Table 1; Suppl. Table 2; Suppl. Fig. 1), suggesting the movement from ^{18}O-depleted to ^{18}O-enriched waters during the analysed period. A third group of three

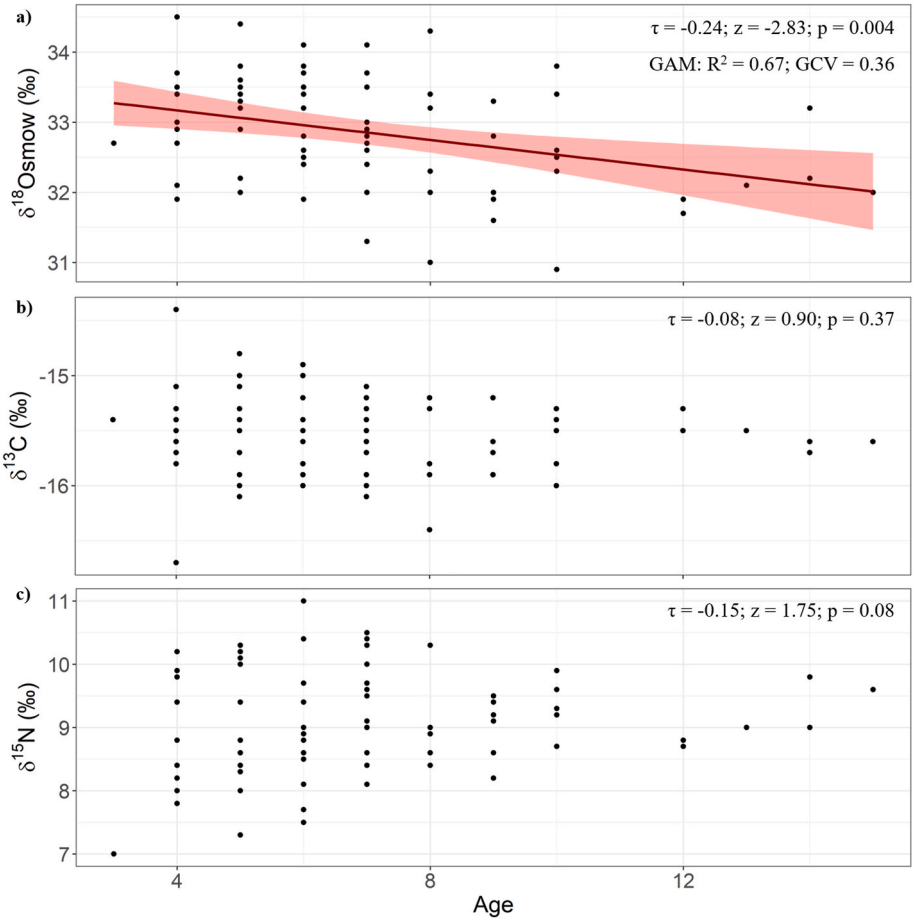

Fig. 3. Individual (a) $\delta^{18}O$, (b) $\delta^{13}C$ and (c) $\delta^{15}N$ values for each of the analysed incremental layer and the respective estimated age (with all individuals pooled together), including the statistics for the Kendall's rank correlation (τ) and a visual representation of the only adjusted generalized additive model (GAM) that showed a good fit (a), with the mean tendency (dark red line) and the respective 95 % confidence interval (light red shaded area).

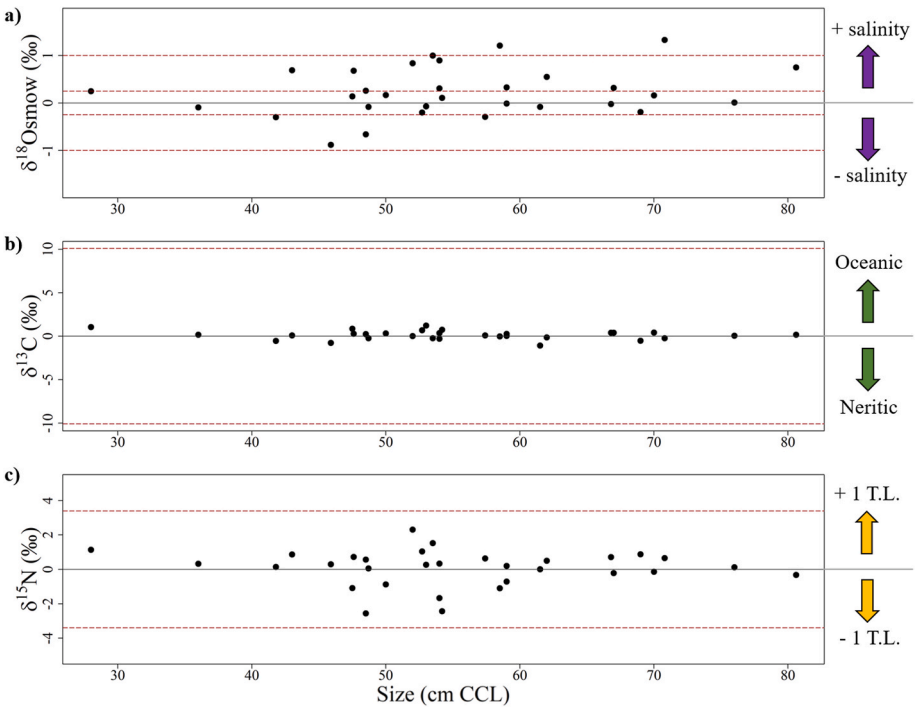

Fig. 4. Differences between the stable isotope ratios of the outermost and the innermost analysed incremental layers for each of the considered loggerhead turtles (n = 31) and their environmental interpretation. Each turtle is represented in each panel by a single black dot. The horizontal solid line within each panel denotes no change over time. The dashed red line at ± 0.25 ‰ in panel "**a**" shows the mean difference between adjacent regions of the Mediterranean Sea and that at ± 1.00 ‰ shows the difference between the Northeast Atlantic Ocean and the eastern Mediterranean Sea (LeGrande and Schmidt, 2006). The dashed red line at ± 10.1 ‰ in panel "**b**" represents the difference between the oceanic particulate organic matter and the neritic seagrass *Posidonia oceanica* off the Balearic Islands (Cardona et al., 2007). The dashed red line at ± 3.4 ‰ in panel "**c**" denotes changes corresponding to one trophic level (T.L.), according to the mean trophic fractionation in aquatic ecosystems (Post, 2002).

turtles (I4, M19, A18) showed the highest $\delta^{18}O$ value in their middle layer and similarly low values in their outermost and innermost incremental layers (Table 1; Suppl. Table 2; Suppl. Fig. 1), indicating the movement from a ^{18}O-depleted to a ^{18}O-enriched region and back to a ^{18}O-depleted region. Finally, the remaining seven turtles had a difference smaller than ±0.25 ‰ between all the analysed incremental layers and hence, they were considered to be similar. This included two of the oldest turtles analysed in this study, A39 and M17, estimated to be 13 and 15 years old, respectively, when stranded. They both showed similarly low $\delta^{18}O$ values between the analysed incremental layers, covering around seven years (from 7 to 13 years old) for the former and nine years (from 7 to 15 years old) for the latter (Table 1; Suppl. Table 2; Suppl. Fig. 1).

In addition to what is mentioned above, five turtles (A19, A15, A13, A28, A22) belonging to the first two groups and with an estimated age between 8 and 13 years old, showed differences larger than ± 1.00 ‰ between at least two of the analysed incremental layers (Table 2; Fig. 4, a), a change that seemed to occur in about two years for four of these individuals (Table 1; Suppl. Table 2; Suppl. Fig. 1).

On the other hand, the $\delta^{13}C$ values obtained for the incremental layers of the considered turtles ranged from −16.7 to −14.4 ‰ (−15.5 ± 0.4 ‰; Suppl. Table 4) and showed no significant correlation with the corresponding estimated age (Kendall's rank correlation: $\tau = -0.08$, $z = -0.90$, $p = 0.37$; Fig. 3, b). In this case, the maximum difference between the highest and the lowest $\delta^{13}C$ values for the analysed incremental layers was 2.3 ‰ and between layers of the same individual was 1.2 ‰, both considerably smaller than the estimated difference between oceanic and neritic habitats in the study area (±10.1 ‰; see Methods; Fig. 4), thus suggesting that all the considered turtles relied on a similar diet which seemed to remain stable during the studied period.

Conversely, the $\delta^{15}N$ values of all incremental layers ranged from 11.04 to 7.05 ‰ (9.1 ± 0.8 ‰; Suppl. Table 5), with less variability and higher values in those over 9 years old (Fig. 3, c). However, no statistically significant correlation was observed between the $\delta^{15}N$ values and the corresponding age (Kendall's rank correlation: $\tau = 0.15$; $z = 1.75$; $p = 0.08$; Fig. 3, c). Here, the maximum difference observed between incremental layers of the same individual was 2.3 ‰ (Suppl. Table 2), which is smaller than the mean estimated trophic enrichment of 3.4 ‰ per trophic level (see Methods; Fig. 4), suggesting no changes in trophic position during the studied period. Nevertheless, the $\delta^{15}N$ values of all samples combined covered a range of about 4.00 ‰, which can suggest that some individuals might be using regions with different $\delta^{15}N$ baselines.

Finally, the standard ellipses of the analysed age classes largely overlapped within the $\delta^{13}C$ - $\delta^{15}N$ isospace, with the ellipses of the youngest age classes encompassing those of the older ones (Fig. 5, a). Furthermore, the standard ellipse area (SEAc) decreased significantly with age (Kendall's rank correlation: $\tau = -0.86$, $z = -2.97$, $p = 0.003$) and the adjusted GAM, which accounted for 89.3 % of the variability in the data, suggested linear relationship between the SEAc and age (GAM model: R^2 (adj) = 0.88, GCV = 0.05, Scale est. = 0.04; Fig. 5, b).

4. Discussion

The evidence here reported revealed that the loggerhead turtles of Northwestern Atlantic origin found dead stranded in the Balearic Islands exhibited a broad variability in the $\delta^{18}O$ values of their bones, both across incremental layers of the same individual and across individuals. Variability was particularly high when turtles were under nine years old and decreased thereafter. These results indicate that the 29 turtles of which an incremental layer younger than 10 years old was identified inhabited a diversity of water masses of different salinities as early juveniles, before settling in lower salinity areas such as the Algerian Basin after reaching 10 years or older. Moreover, the temporal pattern of

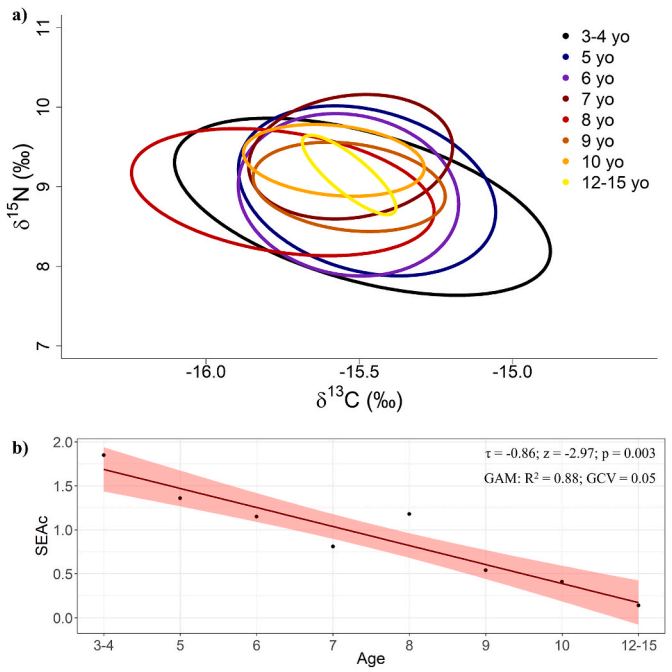

Fig. 5. a) Standard ellipses containing 40 % of the data within the $\delta^{13}C$ - $\delta^{15}N$ isospace of eight age classes of loggerhead turtles observed in the study. Individual values are not shown. Sample sizes are as follows: 3–4 years old (n = 10), 5 years old (n = 12), 6 years old (n = 14), 7 years old (n = 14), 8 years old (n = 6), 9 years old (n = 6), 10 years old (n = 6), and 12–15 years old (n = 6). **b)** Relationship between the standard ellipse area corrected for small sample size (SEAc) from the top panel and the estimated age, showing the statistics for the Kendall's rank correlation (τ) and a visual representation of the adjusted generalized additive model (GAM), with the mean trend (dark red line) and the respective 95 % confidence interval (light red shaded area).

change was also extremely variable, suggesting that the entry to the Mediterranean Sea may happen at any time after their arrival to the Northeast Atlantic Ocean. On the other hand, the $\delta^{13}C$ and $\delta^{15}N$ values of the incremental layers also exhibited a broader variability during the first 6 years of life, although mean values suggested only minor ontogenetic changes in the diet during the analysed period.

4.1. The $\delta^{18}O$ in Mediterranean surface waters

The loggerhead turtles analysed in the present study exhibited four major patterns of individual movement during the time recorded in the cortical bone of the humerus: 1) movement from ^{18}O-enriched to ^{18}O-depleted waters (n = 17), with some of them (n = 4) returning to ^{18}O-enriched waters; 2) movement from ^{18}O-depleted to ^{18}O-enriched waters (n = 4), which is the expected pattern from turtles that recently entered the Mediterranean Sea from the Northeast Atlantic Ocean (Fig. 1); 3) movement from ^{18}O-depleted to ^{18}O-enriched and back to ^{18}O-depleted waters (n = 3), and 4) long-term residence in ^{18}O depleted waters (n = 7).

As described in the introduction, water circulation in the Mediterranean Sea is mostly driven by an excess of evaporation over precipitation and river runoff, which results in a decrease of sea level inside the Mediterranean and the permanent eastward flow of surface water from the Atlantic through the Strait of Gibraltar (Millot et al., 2005). The constant input of less salty Atlantic waters to the west and the higher evaporation rate of surface waters to the east due to higher environmental temperatures, create a marked and predictable salinity gradient that allows to divide the Mediterranean Sea into four regions as follows: (1) Strait of Gibraltar and Alboran Sea, (2) western basin, (3) central basin, and (4) eastern basin (Fig. 1). Furthermore, the preferential evaporation of water molecules carrying ^{16}O atoms causes a local enrichment of ^{18}O in seawater (Sharp, 2017), producing a positive and linear correlation between the salinity and the $\delta^{18}O$ ratio in surface waters (Conroy et al., 2014; Belem et al., 2019) and thus allowing the isotopic distinction between water masses.

According to the estimations made by LeGrande & Smith (LeGrande and Schmidt, 2006) and represented in Fig. 1, the $\delta^{18}O$ values of Mediterranean surface waters show a similar gradual increase from the Strait of Gibraltar towards the eastern basin as the salinity, with a mean increase of 0.25 ‰ from one region to the next. Hence, if the difference in $\delta^{18}O$ values across the incremental layers of a turtle is larger than this absolute value, it can be an indicative of movement between regions with different salinities. Moreover, a mean increase of 1.00 ‰ or larger represents the absolute difference between Atlantic waters and the eastern Mediterranean (LeGrande and Schmidt, 2006) and hence, if this was the only source of variability for the $\delta^{18}O$ values of bone tissue, the expected range of $\delta^{18}O$ values in the incremental layers of the population should be equal or lower than 1.00 ‰.

4.2. Variability of $\delta^{18}O$ between incremental layers

In this context, 24 out of the 31 considered turtles showed differences equal or larger than 0.25 ‰ between incremental layers (Table 1; Suppl. Table 2), with six individuals (A10, M11, A20, A35, I4, A18) having the lowest $\delta^{18}O$ values in their outermost layer. Three of these turtles died when they were six or seven years old and hence, they would have had to cross the Atlantic Ocean and reach the saltier regions of the Mediterranean Sea in less than four years after birth, stranding at the Balearic Islands after spending at least one year in a less salty region. The plausibility of that trip is supported by satellite telemetry data from previous studies. First, Lagrangian drifters indicate that the trans-Atlantic drift time for early juvenile turtles from the Northwest Atlantic found in the United Kingdom was between 1.80 and 3.75 years (Hays and Marsh, 1997). Second, satellite-tracked head-started early juveniles ranging 12.8–19.9 cm CCL and 3.5–9 months old spent less than one year to reach the Azores after being released off southeast Florida (Mansfield et al., 2014). Third, some satellite-tracked head-started early juveniles ranging 18.1–25.0 cm CCL and 9–13 months old released off Spain drifted into the eastern Mediterranean after only a few months, although most individuals remained within the western Mediterranean (Abalo-Morla et al., 2023). This evidence suggests that loggerhead turtles from the Northwest Atlantic Ocean can potentially reach the eastern Mediterranean Sea in less than four years, thus supporting the interpretation stated above. On the other hand, the permanent eastward flow of surface water in the Channel of Sicily may retain them within the central and eastern basins until they grow large enough to swim counter-current (Cardona and Hays, 2018). This would explain why all the loggerhead turtles analysed here with evidence of re-entering the western Mediterranean from the eastern basin are larger than 40 cm CCL, the minimum carapace length required to swim counter-current along the Channel of Sicily (Cardona and Hays, 2018).

On the contrary, 17 individuals between 5 and 13 years old had the highest $\delta^{18}O$ values in the outermost incremental layer, yet they were all recovered dead off the Balearic Islands, indicating that they moved from a less salty region several months before their death. However, only three of those turtles showed evidence of the use of saltier areas in older-age incremental layers, whereas for the remaining 14 individuals, the pattern is consistent with an arrival to the western Mediterranean from the Atlantic between the formation of the innermost and the outermost incremental layers. Furthermore, five individuals (A19, A15, A13, A28 and A22) between 8 and 13 years old showed differences large enough (+1.00 ‰) to indicate movement from areas with high influence of Atlantic waters towards the saltiest parts of the eastern Mediterranean. Three of them (A15, A13, A28) showed this large difference twice in the analysed periods, probably changing regions every two years, approximately, and seemingly moving from the eastern to the western basin and back.

In addition, two of the oldest turtles of the study (A39 and M17; 70.0 and 76.0 cm CCL, respectively), estimated to be 13 and 15 years old when stranded, were the only ones that showed similarly low $\delta^{18}O$ values for the whole analysed period, which in this case corresponded to the last seven and nine years, respectively, before stranding. This is a strong indication of several years of foraging in the southern part of the western Mediterranean, likely at the Algerian Basin, and is consistent with the use of these area as an important foraging ground for the species, as revealed recently through satellite telemetry of 103 loggerhead turtles which included post-hatchlings, juveniles and adults of both sexes (22.8–83.0 cm CCL) (Abalo-Morla et al., 2022).

Finally, amongst all the $\delta^{18}O$ values obtained here, there were three notably lower than the rest. Two of them corresponded to the innermost sampled layers of two different individuals (A26 and A22) from when they were eight and nine years old. Hence, it is possible that these low values correspond to their time in the Atlantic Ocean, in which case they would have delayed their entrance to the Mediterranean Sea after spending several years in the eastern Atlantic. By contrast, the third low value belonged to the middle layer of turtle A15, and the values of the innermost and the outermost sampled layers of this individual were distinctively higher, with a difference of −1.76 and + 1.57 ‰, respectively, which is much larger than the estimated for the Mediterranean basin (±1.00 ‰). Similar changes were also found in other three turtles (+1.82 ‰, +1.48 ‰ and +1.33 ‰ for turtles A13, A28 and A22, respectively), which suggests that there are likely other factors affecting the $\delta^{18}O$ values of bone carbonate in loggerhead turtles. These factors are discussed in the next section.

4.3. Sources of variability in bone $\delta^{18}O$ values

An important shortcoming to consider is that the isotopic composition of seawater is not the only factor influencing the isotopic values of bone tissue in sea turtles. The $\delta^{18}O$ value of bone carbonate (bioapatite) is given by that of the body water from which carbonate precipitates, which depends on the magnitude and isotopic composition of the different oxygen fluxes into and out of the body, the isotopic fractionations associated with metabolism, and the temperature at which it forms (Kohn, 1996; Kohn and Cerling, 2002; Luz et al., 1984).

Sea turtles have two main sources of oxygen that can influence the $\delta^{18}O$ values of their tissues. One is the metabolic water produced through cellular respiration using the atmospheric O_2, which is enriched in ^{18}O compared to seawater due to the Dole effect (Luz and Barkan, 2011; Luz et al., 1984), and the other one is the ingested seawater, either by direct drinking or from their prey (Jones et al., 2009). Given that sea turtles drink seawater regularly (Reina et al., 2002) and the diet of oceanic loggerhead turtles is dominated by jelly plankton with a very high water content (Cardona et al., 2012), the contribution of metabolic water to the body water of sea turtles is minimal (Jones et al., 2009) and therefore, the $\delta^{18}O$ values of bone carbonate are expected to reflect mostly those of the water mass where they live (Séon et al., 2023). Nevertheless, the range of $\delta^{18}O$ values reported here for the analysed loggerhead turtles is much broader than the range expected for seawater within the study area (3.60 vs 1.00 ‰, respectively). Furthermore, the difference between adjacent incremental layers was, in some cases, as large as 1.82 ‰, also much larger than the estimated range of variability within the whole Mediterranean basin and the adjoining Atlantic Ocean (1.30 ‰). This leads to the conclusion that other processes must be affecting the $\delta^{18}O$ values during the formation of bone carbonate in sea turtles.

The $\delta^{18}O$ fractionation factor between body water and carbonate during bioapatite precipitation is temperature dependent (Sharp, 2017; Coulson et al., 2008) when isotopic equilibrium between carbonate and water is reached (Kim and O'Neil, 1997). Due to the ectothermic nature of turtles, at higher environmental temperatures their body temperature also increases, causing a decrease in the carbonate-water fractionation factor during bioapatite precipitation and producing carbonates with a more similar ^{18}O content to that of the body water used during precipitation (Kohn and Cerling, 2002; Kim and O'Neil, 1997), which in this case is primarily the ^{18}O-enriched ingested seawater. Another consequence of the increased body temperature, assuming a regular food and water intake, is an increase in the metabolic rate of the turtle and, therefore, in the turnover rate of body water, which can accelerate bioapatite precipitation (i.e., bone tissue grows faster) and in turn affect the isotopic balance between body water and carbonate, producing bioapatite out of isotopic equilibrium with body water. In this case, the reaction becomes less dependent on the temperature and could alter the resultant $\delta^{18}O$ values (Kim and O'Neil, 1997).

On the contrary, the exposure to cold temperatures causes a significant reduction on the metabolic rate, food intake and O_2 consumption in sea turtles (Hochscheid et al., 2004). In this case, the turnover rate of body water and thus the precipitation of bioapatite will be slower and more likely to reach isotopic equilibrium with body water. Hence, if food and water intake are not limiting and the evaporation rate in surface waters is lower due to lower temperatures, the bioapatite produced during this period will likely have lower $\delta^{18}O$ values than that produced in warmer waters (Kim and O'Neil, 1997).

On the other hand, if the turtle remains in a state of low metabolic activity due to low food availability, or even reach a fasting state, the effect over the $\delta^{18}O$ values of bioapatite will be the opposite. Oceanic juvenile loggerhead turtles alternate periods of high food availability with extended periods of fasting (Bjorndal et al., 2003), during which they rely on their fat stores to obtain energy (Jones et al., 2009) and thus, metabolic water is expected to become the dominant influx of water in their bodies unless they increase the drinking rate. As mentioned above, metabolic water is enriched in ^{18}O compared to seawater (Luz and Barkan, 2011) and animals relying on lipid-rich diets, as well as those with irregular access to food or subjected to fasting, tend to be enriched in ^{18}O (Jones et al., 2009; Séon et al., 2023). In addition, the eastern Mediterranean is highly oligotrophic (Bosc et al., 2004), which results in a scarcity of oceanic loggerhead turtles in the area (DiMatteo et al., 2022). Therefore, if the juvenile loggerhead turtles of Northwestern Atlantic origin entering the eastern Mediterranean (Clusa et al., 2014) have less access to food and fast more frequently than those remaining in the western Mediterranean, they would exhibit an additional increase in their $\delta^{18}O$ values, operating in synergy with a higher sea surface temperature and evaporation rate (measured as salinity) in the eastern basin (Millot et al., 2005) to considerably expand the range of $\delta^{18}O$ values in bone carbonate compared to seawater.

From the above follows that regional differences in water temperature and food availability may have an impact on the $\delta^{18}O$ values of sea turtle's bone carbonate, since they both affect the metabolic rate and hence, the turnover rate of the body water used in bioapatite precipitation. In the Mediterranean Sea, salinity, sea surface temperature and food availably change along the west-east axis, reinforcing the eastward increase in the $\delta^{18}O$ values of sea turtles bone carbonate, but this is not necessarily true elsewhere. Thus, researchers should keep in mind these other sources of variability when using $\delta^{18}O$ as a habitat tracer in sea turtles. Another caveat to be considered is that incremental layers formed during fasting periods are narrower than those formed in feasting periods and hence contribute with a smaller amount of carbonate when assessing the $\delta^{18}O$ value of samples integrating several incremental layers.

4.4. Trophic ecology according to bone $\delta^{13}C$ and $\delta^{15}N$

In general, the changes observed in the $\delta^{13}C$ and $\delta^{15}N$ values between incremental layers were small and suggested only minor ontogenetic changes in the diet of these juvenile loggerhead turtles during their journey through the Mediterranean Sea, with a tendency to reduce the isotopic niche area as they grow older. This is consistent with movement patterns previously observed for loggerhead turtles in the Mediterranean Sea, as the movement of turtles smaller than 40 cm CCL is highly

dependent on current velocity (Revelles et al., 2007a), whereas larger turtles can actively remain in more favourable areas (Eckert et al., 2008).

Considering that the bone samples used in the present study are from the early 2000's, we considered the environmental conditions of the Mediterranean Sea of that time for the following discussions. On one hand, the range of $\delta^{13}C$ values obtained for the considered turtles (from −16.7 to −14.4 ‰) is consistent to that of potential pelagic prey such as gelatinous plankton (from −17.6 to −15.7 ‰) and small pelagic and mesopelagic fishes (from −16.4 to −15.9 ‰) from foraging grounds off the Balearic Islands (Cardona et al., 2007), after accounting for the diet-to-tissue fractionation reported for the cortical bone of sea turtles (2.1 ± 0.6 ‰) (Turner Tomaszewicz et al., 2017b). This similarity suggests the use of mostly oceanic habitats. Furthermore, the variability observed between individuals could be explained by the horizontal distribution of $\delta^{13}C$ values in surface waters within and between Mediterranean basins. Pierre (1999) found that the northern margins of both the eastern and western Mediterranean, known as regions of deep-water formation, present the lowest $\delta^{13}C$ values because of the input of ^{13}C-depleted CO_2 from deeper waters especially during winter, whereas the highest values are found in the Alboran Sea and southern Algerian Basin. However, the range of values in both basins was similar and the maximum differences reported for the western and eastern Mediterranean were small (0.43 and 0.41 ‰, respectively) (Pierre, 1999), which explains the little variability observed in our data.

Regarding the $\delta^{15}N$ values, those of the studied loggerhead turtles ranged between 7.05 and 11.04 ‰ and stomach content analysis of pelagic loggerhead turtles off the Balearic Islands had previously revealed gelatinous plankton and pelagic fishes as their main prey (Revelles et al., 2007b). The $\delta^{15}N$ values of gelatinous plankton from the Balearic Islands in the early 2000's ranged 3.9–5.6 ‰ and those of small pelagic and mesopelagic fishes from the same area and period ranged 8.7–10.2 ‰ (Cardona et al., 2007). As the diet-to-tissue discrimination factor for the cortical bone of sea turtles is 5.1 ± 1.1 ‰ (Eckert et al., 2008), the $\delta^{15}N$ of the diet of loggerhead turtles should range 1.95–5.4 ‰, suggesting that gelatinous zooplankton was the staple food of the loggerhead turtles analysed during the life stages recorded in their bone tissue, a conclusion consistent with the results of a previous mixing model based on the $\delta^{13}C$ and $\delta^{15}N$ values of epidermis (Cardona et al., 2007). Another possibility is that these differences are caused by the higher $\delta^{15}N$ values of the particulate organic matter in the surface waters of the western basin, especially towards the Alboran Sea (Pantoja et al., 2002). If this was the case, it would agree with the previously discussed tendency to settle in areas of lower salinity of the western Mediterranean as they reach ten years of age.

Lastly, the tendency to reduce the isotopic niche area is mostly driven by a lower variability in incremental layers older than 9 years old. This indicates either a more consistent diet over time, a greater fidelity to the same water mass, or both, in older turtles.

5. Conclusions

Our results suggest that loggerhead turtles born at the nesting beaches of the Northwest Atlantic do not follow just one straight path towards the Mediterranean Sea, and the wide range of $\delta^{18}O$ values found for these turtles, especially in those younger than nine years old, do not indicate any specific temporal patter in their movements. This agrees with the observations of Mansfield et al. (2014), where some satellite tracked neonate loggerhead turtles released off their natal beaches in Florida travelled out of the Gulf Stream and towards the Sargasso Sea in association with meso-scale eddies and remained there for different periods of time, while others seemed to swim directly towards the eastern Atlantic (Mansfield et al., 2014). This uneven dispersion of neonates while crossing the Atlantic explains the non-systematic entry of juvenile loggerhead turtles into the Mediterranean Sea as well as the variability of $\delta^{18}O$ values in turtles of similar size and age. Similar variations in the timing of ontogenic habitat shifts were observed in juvenile loggerhead turtles from the North Pacific (Turner Tomaszewicz et al., 2017a). Moreover, the observed tendency to settle in lower salinity areas as they grow older than 10 years old does not seem to be related to their distribution as juveniles. Available satellite data suggests that individuals larger than 57 cm CCL are more likely to remain within the Alboran Sea and the adjacent Algerian Basin (Eckert et al., 2008), and they can already leave the Mediterranean and start their journey back to the Northwestern Atlantic before reaching 68 cm CCL (Moncada et al., 2010). According to our estimations, all turtles estimated to be 10 years or older had a CCL larger than 57 cm. Certainly, the exact time of their departure is highly variable and likely depends on factors that are mostly unknown but may include the availability of food resources and good environmental conditions (Eckert et al., 2008).

CRediT authorship contribution statement

Alessandra Cani: Writing – original draft, Visualization, Validation, Software, Methodology, Investigation, Formal analysis, Data curation, Conceptualization. **Cristina Besén:** Writing – original draft, Software, Methodology, Investigation, Formal analysis, Data curation. **Carlos Carreras:** Writing – original draft, Validation, Software, Resources, Methodology, Investigation, Funding acquisition, Formal analysis, Data curation. **Marta Pascual:** Writing – original draft, Validation, Software, Resources, Methodology, Investigation, Funding acquisition, Formal analysis, Data curation. **Luis Cardona:** Writing – original draft, Visualization, Validation, Supervision, Software, Resources, Project administration, Methodology, Investigation, Funding acquisition, Formal analysis, Data curation, Conceptualization.

Funding

This research was funded with Project GCL2009-10017 by Ministerio de Ciencia, Innovación y Universidades, Spain. AC was supported by Universitat de Barcelona through the PREDOCS-UB grant. MP and CC are members of the research group SGR2021-01271 funded by the Generalitat de Catalunya.

Declaration of competing interest

The authors declare the following financial interests/personal relationships which may be considered as potential competing interests: Luis Cardona reports financial support was provided by Ministerio de Ciencia, Innovación y Universidades, Spain. If there are other authors, they declare that they have no known competing financial interests or personal relationships that could have appeared to influence the work reported in this paper.

Acknowledgements

The authors thank Gloria Fernández for her involvement in the collection of the samples. We also thank the staff of the Centres Científics i Tecnològics (CCiT-UB) of the University of Barcelona (Spain) for their assistance with the stable isotope analysis.

Appendix A. Supplementary data

Supplementary data to this article can be found online at https://doi.org/10.1016/j.marenvres.2024.106851.

Data availability

Data will be made available on request.

References

Abalo-Morla, S., Belda, E.J., March, D., Revuelta, O., Cardona, L., Giralt, S., Crespo-Picazo, J.L., Hochscheid, S., Marco, A., Merchán, M., Sagarminaga, R., 2022. Assessing the use of marine protected areas by loggerhead sea turtles (Caretta caretta) tracked from the western Mediterranean. Global Ecology and Conservation 38, e02196. https://doi.org/10.1016/j.gecco.2022.e02196.

Abalo-Morla, S., Muñoz-Mas, R., Tomás, J., Belda, E.J., 2023. Factors driving dispersal and habitat use of loggerhead sea turtle post-hatchlings and its conservational implications. Marine Biology 170 (12), 155. https://doi.org/10.1007/s00227-023-04285-2.

Belem, A.L., Caricchio, C., Albuquerque, A.L.S., Venancio, I.M., Zucchi, M., Santos, T.H. R., Alvarez, Y.G., 2019. Salinity and stable oxygen isotope relationship in the Southwestern Atlantic: constraints to paleoclimate reconstructions. An Acad. Bras Ciências 91, e20180226. https://doi.org/10.1590/0001-3765201920180226.

Ben-David, M., Flaherty, E.A., 2012. Stable isotopes in mammalian research: a beginner's guide. J. Mammal. 93 (2), 312–328. https://doi.org/10.1644/11-MAMM-S-166.1.

Bjorndal, K.A., Bolten, A.B., Martins, H.R., 2000. Somatic growth model of juvenile loggerhead sea turtles Caretta caretta: duration of pelagic stage. Mar. Ecol. Prog. Ser. 202, 265–272. https://doi.org/10.3354/meps202265.

Bjorndal, K.A., Bolten, A.B., Dellinger, T., Delgado, C., Martins, H.R., 2003. Compensatory growth in oceanic loggerhead sea turtles: response to a stochastic environment. Ecology 84 (5), 1237–1249. https://doi.org/10.1890/0012-9658(2003)084[1237:CGIOLS]2.0.CO;2.

Bolten, A.B., 2003. Active swimmers-passive drifters: the oceanic juvenile stage of loggerheads in the Atlantic system. In: Bolten, A.B., Witherington, B.E. (Eds.), Loggerhead Sea Turtles. Smithsonian Institution Press, Washington, D.C., pp. 63–78

Bosc, E., Bricaud, A., Antoine, D., 2004. Seasonal and interannual variability in algal biomass and primary production in the Mediterranean Sea, as derived from 4 years of SeaWiFS observations. Global Biogeochem. Cycles 18 (1), 1–17. https://doi.org/10.1029/2003GB002034. GB1005.

Brasseur, P., Beckers, J.M., Brankart, J.M., Schoenauen, R., 1996. Seasonal temperature and salinity fields in the Mediterranean Sea: climatological analyses of a historical data set. Deep Sea Res. Oceanogr. Res. Pap. 43 (2), 159–192. https://doi.org/10.1016/0967-0637(96)00012-X.

Cani, A., Cardona, L., Aguilar, Á., Borrell, A., Drago, M., 2024. Fine-tuning the isotopic niche of a marine mammal community through a multi-element approach and variable spatial scales. Estuar. Coast Shelf Sci. 298, 108641. https://doi.org/10.1016/j.ecss.2024.108641.

Cardiff, R.D., Miller, C.H., Munn, R.J., 2014. Manual hematoxylin and eosin staining of mouse tissue sections. Cold Spring Harbor Protocols 2014 (6), 655–658. https://doi.org/10.1101/pdb.prot073411.

Cardona, L., Hays, G.C., 2018. Ocean currents, individual movements and genetic structuring of populations. Marine biology 165, 1–10. https://doi.org/10.1007/s00227-017-3262-2.

Cardona, L., Revelles, M., Sales, M., Aguilar, A., Borrell, A., 2007. Meadows of the seagrass *Posidonia oceanica* are a significant source of organic matter for adjoining ecosystems. Mar. Ecol. Prog. Ser. 335, 123–131. https://doi.org/10.3354/meps335123.

Cardona, L., Álvarez de Quevedo, I., Borrell, A., Aguilar, A., 2012. Massive consumption of gelatinous plankton by Mediterranean apex predators. PLoS One 7 (3), e31329. https://doi.org/10.1371/journal.pone.0031329.

Cardona, L., Clusa, M., Eder, E., Demetropoulos, A., Margaritoulis, D., Rees, A.F., Hamza, A.A., Khalil, M., Levy, Y., Türkozan, O., Marín, I., Aguilar, A., 2014. Distribution patterns and foraging ground productivity determine clutch size in Mediterranean loggerhead turtles. Mar. Ecol. Prog. Ser. 497, 229–241. https://doi.org/10.3354/meps10595.

Cardona, L., Abalo-Morla, S., Cani, A., Feliu-Tena, B., Izaguirre, N., Tomás, J., Belda, E.J., 2024. Identifying the foraging grounds of the new loggerhead turtle nesters in the western Mediterranean. Aquat. Conserv. Mar. Freshw. Ecosyst. 34 (1), e4059. https://doi.org/10.1002/aqc.4059.

Carreras, C., Pascual, M., Tomás, J., Marco, A., Hochscheid, S., Castillo, J.J., Gozalbes, P., Parga, M., Piovano, S., Cardona, L., 2018. Sporadic nesting reveals long distance colonisation in the philopatric loggerhead sea turtle (*Caretta caretta*). Sci. Rep. 8 (1), 1435. https://doi.org/10.1038/s41598-018-19887-w.

Casale, P., Broderick, A.C., Camiñas, J.A., Cardona, L., Carreras, C., Demetropoulos, A., Fuller, W.J., Godley, B.J., Hochscheid, S., Kaska, Y., Lazar, B., 2018. Mediterranean Sea turtles: current knowledge and priorities for conservation and research. Endanger. Species Res. 36, 229–267. https://doi.org/10.3354/esr00090.

Chambault, P., Baudena, A., Bjorndal, K.A., Santos, M.A., Bolten, A.B., Vandeperre, F., 2019. Swirling in the ocean: immature loggerhead turtles seasonally target old anticyclonic eddies at the fringe of the North Atlantic gyre. Prog. Oceanogr. 175, 345–358. https://doi.org/10.1016/j.pocean.2019.05.005.

Chambault, P., Gaspar, P., Dell'Amico, F., 2021. Ecological trap or favorable habitat? First evidence that immature sea turtles may survive at their range-limits in the North-East Atlantic. Front. Mar. Sci. 8, 736604. https://doi.org/10.3389/fmars.2021.736604.

Clusa, M., Carreras, C., Pascual, M., Gaughran, S.J., Piovano, S., Giacoma, C., Fernández, G., Levy, Y., Tomás, J., Raga, J.A., Maffucci, F., 2014. Fine-scale distribution of juvenile atlantic and mediterranean loggerhead turtles (*Caretta caretta*) in the Mediterranean Sea. Marine Biology 161, 509–519. https://doi.org/10.1007/s00227-013-2353-y.

Conroy, J.L., Cobb, K.M., Lynch-Stieglitz, J., Polissar, P.J., 2014. Constraints on the salinity–oxygen isotope relationship in the central tropical Pacific Ocean. Mar. Chem. 161, 26–33.

Coulson, A.B., Kohn, M.J., Shirley, M.H., Joyce, W.G., Barrick, R.E., 2008. Phosphate–oxygen isotopes from marine turtle bones: ecologic and paleoclimatic applications. Palaeogeogr. Palaeoclimatol. Palaeoecol. 264 (1–2), 78–84. https://doi.org/10.1016/j.palaeo.2008.04.008.

de Quevedo, I.Á., San Félix, M., Cardona, L., 2013. Mortality rates in by-caught loggerhead turtle Caretta caretta in the Mediterranean Sea and implications for the Atlantic populations. Mar. Ecol. Prog. Ser. 489, 225–234. https://doi.org/10.3354/meps10411.

DiMatteo, A., Cañadas, A., Roberts, J., Sparks, L., Panigada, S., Boisseau, O., Moscrop, A., Fortuna, C.M., Lauriano, G., Holcer, D., Peltier, H., 2022. Basin-wide estimates of loggerhead turtle abundance in the Mediterranean Sea derived from line transect surveys. Front. Mar. Sci. 9, 930412. https://doi.org/10.3389/fmars.2022.930412.

Durfort, M., 1987. Algunes tècniques d'obtenció de preparacions d'estructures i de teixits animals. Seminaris d'Estudis Universitaris. Institució Catalana d'Història Natural, p. 27.

Eckert, S.A., Moore, J.E., Dunn, D.C., van Buiten, R.S., Eckert, K.L., Halpin, P.N., 2008. Modeling loggerhead turtle movement in the Mediterranean: importance of body size and oceanography. Ecol. Appl. 18 (2), 290–308. https://doi.org/10.1890/06-2107.1.

Fofonoff, N.P., 1981. Chapter 4: the Gulf Stream. In: Warren, B.A., Wunsch, C. (Eds.), Evolution of Physical Oceanography: Scientific Surveys in Honor of Henry Stommel, pp. 112–139.

Frazão, H.C., Prien, R.D., Schulz-Bull, D.E., Seidov, D., Waniek, J.J., 2022. The forgotten Azores current: a long-term perspective. Front. Mar. Sci. 9, 842251. https://doi.org/10.3389/fmars.2022.842251.

Freitas, C., Caldeira, R., Dellinger, T., 2019. Surface behavior of pelagic juvenile loggerhead sea turtles in the eastern North Atlantic. Journal of experimental marine biology and ecology 510, 73–80. https://doi.org/10.1016/j.jembe.2018.10.006.

Gat, J.R., 1996. Oxygen and hydrogen isotopes in the hydrologic cycle. Annu. Rev. Earth Planet Sci. 24 (1), 225–262.

Goshe, L.R., Avens, L., Snover, M.L., Hohn, A.A., 2020. Protocol for processing sea turtle bones for age estimation. NOAA Technical Memorandum NMFS-SEFSC-746. U.S. Department of Commerce, p. 43. https://doi.org/10.25923/gqva-9y22.

Hays, G.C., Marsh, R., 1997. Estimating the age of juvenile loggerhead sea turtles in the North Atlantic. Can. J. Zool. 75 (1), 40–46. https://doi.org/10.1139/z97-005.

Hochscheid, S., Bentivegna, F., Speakman, J.R., 2004. Long-term cold acclimation leads to high Q10 effects on oxygen consumption of loggerhead sea turtles Caretta caretta. Physiol. Biochem. Zool. 77 (2), 209–222. https://doi.org/10.1086/381472.

Jackson, A.L., Inger, R., Parnell, A.C., Bearhop, S., 2011. Comparing isotopic niche widths among and within communities: SIBER Stable Isotope Bayesian Ellipses in R. J. Anim. Ecol. 80 (3), 595–602.

Jones, T.T., Hastings, M.D., Bostrom, B.L., Andrews, R.D., Jones, D.R., 2009. Validation of the use of doubly labeled water for estimating metabolic rate in the green turtle (*Chelonia mydas* L.): a word of caution. J. Exp. Biol. 212 (16), 2635–2644. https://doi.org/10.1242/jeb.029330.

Kim, S.T., O'Neil, J.R., 1997. Equilibrium and nonequilibrium oxygen isotope effects in synthetic carbonates. Geochem. Cosmochim. Acta 61 (16), 3461–3475. https://doi.org/10.1016/S0016-7037(97)00169-5.

Koch, P.L., Tuross, N., Fogel, M.L., 1997. The effects of sample treatment and diagenesis on the isotopic integrity of carbonate in biogenic hydroxyapatite. J. Archaeol. Sci. 24 (5), 417–429. https://doi.org/10.1006/jasc.1996.0126.

Kohn, M.J., 1996. Predicting animal δ18O: accounting for diet and physiological adaptation. Geochem. Cosmochim. Acta 60 (23), 4811–4829. https://doi.org/10.1016/S0016-7037(96)00240-2.

Kohn, M.J., Cerling, T.E., 2002. Stable isotope compositions of biological apatite. Rev. Mineral. Geochem. 48 (1), 455–488. https://doi.org/10.2138/rmg.2002.48.12.

LeGrande, A.N., Schmidt, G.A., 2006. Global gridded data set of the oxygen isotopic composition in seawater. Geophys. Res. Lett. 33 (12), 1–5. https://doi.org/10.1029/2006GL026011.

Lohmann, K.J., Cain, S.D., Dodge, S.A., Lohmann, C.M., 2001. Regional magnetic fields as navigational markers for sea turtles. Science 294 (5541), 364–366. https://doi.org/10.1126/science.1064557.

Lohmann, K.J., Putman, N.F., Lohmann, C.M., 2012. The magnetic map of hatchling loggerhead sea turtles. Curr. Opin. Neurobiol. 22 (2), 336–342. https://doi.org/10.1016/j.conb.2011.11.005.

Luna-Ortiz, A., Marín-Capuz, G., Abella, E., Crespo-Picazo, J.L., Escribano, F., Félix, G., Giralt, S., Tomás, J., Pegueroles, C., Pascual, M., Carreras, C., 2024. New colonisers drive the increase of the emerging loggerhead turtle nesting in Western Mediterranean. Sci. Rep. 14 (1), 1506. https://doi.org/10.1038/s41598-024-51664-w.

Luz, B., Barkan, E., 2011. The isotopic composition of atmospheric oxygen. Global Biogeochem. Cycles 25 (3), 14. https://doi.org/10.1029/2010GB003883.

Luz, B., Kolodny, Y., Horowitz, M., 1984. Fractionation of oxygen isotopes between mammalian bone-phosphate and environmental drinking water. Geochem. Cosmochim. Acta 48 (8), 1689–1693. https://doi.org/10.1016/0016-7037(84)90338-7.

Mansfield, K.L., Saba, V.S., Keinath, J.A., Musick, J.A., 2009. Satellite tracking reveals a dichotomy in migration strategies among juvenile loggerhead turtles in the Northwest Atlantic. Marine Biology 156, 2555–2570. https://doi.org/10.1007/s00227-009-1279-x.

Mansfield, K.L., Wyneken, J., Porter, W.P., Luo, J., 2014. First satellite tracks of neonate sea turtles redefine the 'lost years' oceanic niche. Proc. Biol. Sci. 281 (1781), 20133039. https://doi.org/10.1098/rspb.2013.3039.

McClellan, C.M., Read, A.J., 2007. Complexity and variation in loggerhead sea turtle life history. Biol. Lett. 3 (6), 592–594. https://doi.org/10.1098/rsbl.2007.0355.

Millot, C., Taupier-Letage, I., 2005. Circulation in the Mediterranean Sea. In: Saliot, A. (Ed.), The Mediterranean Sea. Handbook of Environmental Chemistry, 5K. Springer, Berlin, Heidelberg, pp. 29–66. https://doi.org/10.1007/b107143.

Moncada, F., Abreu-Grobois, F.A., Bagley, D., Bjorndal, K.A., Bolten, A.B., Camiñas, J.A., Ehrhart, L., Muhlia-Melo, A., Nodarse, G., Schroeder, B.A., Zurita, J., 2010. Movement patterns of loggerhead turtles Caretta caretta in Cuban waters inferred from flipper tag recaptures. Endanger. Species Res. 11 (1), 61–68. https://doi.org/10.3354/esr00248.

Monzón-Argüello, C., Rico, C., Carreras, C., Calabuig, P., Marco, A., López-Jurado, L.F., 2009. Variation in spatial distribution of juvenile loggerhead turtles in the eastern Atlantic and western Mediterranean Sea. J. Exp. Mar. Biol. Ecol. 373 (2), 79–86. https://doi.org/10.1016/j.jembe.2009.03.007.

Newsome, S.D., Clementz, M.T., Koch, P.L., 2010. Using stable isotope biogeochemistry to study marine mammal ecology. Mar. Mamm. Sci. 26 (3), 509–572. https://doi.org/10.1111/j.1748-7692.2009.00354.x.

Palter, J.B., 2015. The role of the Gulf Stream in European climate. Ann. Rev. Mar. Sci 7, 113–137. https://doi.org/10.1146/annurev-marine-010814-015656.

Pantoja, S., Repeta, D.J., Sachs, J.P., Sigman, D.M., 2002. Stable isotope constraints on the nitrogen cycle of the Mediterranean Sea water column. Deep Sea Res. Oceanogr. Res. Pap. 49 (9), 1609–1621. https://doi.org/10.1016/S0967-0637(02)00066-3.

Parham, J.F., Zug, G.R., 1997. Age and growth of loggerhead sea turtles (Caretta caretta) of coastal Georgia: an assessment of skeletochronological age-estimates. Bull. Mar. Sci. 61 (2), 287–304.

Piecuch, C.G., Beal, L.M., 2023. Robust weakening of the Gulf Stream during the past four decades observed in the Florida Straits. Geophys. Res. Lett. 50 (18), e2023GL105170. https://doi.org/10.1029/2023GL105170.

Pierre, C., 1999. The oxygen and carbon isotope distribution in the Mediterranean water masses. Mar. Geol. 153 (1–4), 41–55. https://doi.org/10.1016/S0025-3227(98)00090-5.

Piovano, S., Clusa, M., Carreras, C., Giacoma, C., Pascual, M., Cardona, L., 2011. Different growth rates between loggerhead sea turtles (*Caretta caretta*) of Mediterranean and Atlantic origin in the Mediterranean Sea. Marine Biology 158, 2577–2587. https://doi.org/10.1007/s00227-011-1759-7.

Post, D.M., 2002. Using stable isotopes to estimate trophic position: models, methods, and assumptions. Ecology 83 (3), 703–718.

R Core Team, 2021. R: A Language and Environment for Statistical Computing. R Foundation for Statistical Computing, Vienna. https://www.R-project.org. (Accessed 26 September 2024).

Ramirez, M.D., Avens, L., Seminoff, J.A., Goshe, L.R., Heppell, S.S., 2015. Patterns of loggerhead turtle ontogenetic shifts revealed through isotopic analysis of annual skeletal growth increments. Ecosphere 6 (11), 1–17. https://doi.org/10.1890/ES15-00255.1.

Ramos, R., González-Solís, J., 2012. Trace me if you can: the use of intrinsic biogeochemical markers in marine top predators. Front. Ecol. Environ. 10 (5), 258–266. https://doi.org/10.1890/110140.

Reina, R.D., Jones, T.T., Spotila, J.R., 2002. Salt and water regulation by the leatherback sea turtle Dermochelys coriacea. J. Exp. Biol. 205 (13), 1853–1860. https://doi.org/10.1242/jeb.205.13.1853.

Revelles, M., Carreras, C., Cardona, L., Marco, A., Bentivegna, F., Castillo, J.J., de Martino, G., Mons, J.L., Smith, M.B., Rico, C., Pascual, M., 2007a. Evidence for an asymmetrical size exchange of loggerhead sea turtles between the Mediterranean and the Atlantic through the Straits of Gibraltar. J. Exp. Mar. Biol. Ecol. 349 (2), 261–271. https://doi.org/10.1016/j.jembe.2007.05.018.

Revelles, M., Cardona, L., Aguilar, A., Fernández, G., 2007b. The diet of pelagic loggerhead sea turtles (Caretta caretta) off the Balearic archipelago (western Mediterranean): relevance of long-line baits. J. Mar. Biol. Assoc. U. K. 87 (3), 805–813. https://doi.org/10.1017/S0025315407054707.

Rubenstein, D.R., Hobson, K.A., 2004. From birds to butterflies: animal movement patterns and stable isotopes. Trends Ecol. Evol. 19 (5), 256–263. https://doi.org/10.1016/j.tree.2004.03.017.

Schmitz, Jr, W, J., McCartney, M.S., 1993. On the north Atlantic circulation. Rev. Geophys. 31 (1), 29–49. https://doi.org/10.1029/92RG02583.

Séon, N., Brasseur, I., Scala, C., Tacail, T., Catteau, S., Fourel, F., Vincent, P., Lécuyer, C., Suan, G., Charbonnier, S., Vinçon-Laugier, A., 2023. Determination of water balance maintenance in Orcinus orca and Tursiops truncatus using oxygen isotopes. J. Exp. Biol. 226 (23), jeb245648. https://doi.org/10.1242/jeb.245648.

Sharp, Z., 2017. Principles of Stable Isotope Geochemistry, second ed. University of New Mexico. https://doi.org/10.25844/h9q1-0p82.

Snover, M.L., Hohn, A.A., Crowder, L.B., y Macko, S.A., 2010. Combining stable isotopes and skeletal growth marks to detect habitat shifts in juvenile loggerhead sea *turtles Caretta caretta*. Endanger. Species Res. 13 (1), 25–31. https://doi.org/10.3354/esr00311.

Soto-Navarro, J., Jordá, G., Amores, Á., Cabos, W., Somot, S., Sevault, F., Macías, D., Djurdjevic, V., Sannino, G., Li, L., Sein, D., 2020. Evolution of Mediterranean Sea water properties under climate change scenarios in the Med-CORDEX ensemble. Clim. Dynam. 54, 2135–2165. https://doi.org/10.1007/s00382-019-05105-4.

Turner Tomaszewicz, C.N., Seminoff, J.A., Ramirez, M.D., Kurle, C.M., 2015. Effects of demineralization on the stable isotope analysis of bone samples. Rapid Commun. Mass Spectrom. 29 (20), 1879–1888. https://doi.org/10.1002/rcm.7295.

Turner Tomaszewicz, C.N., Seminoff, J.A., Peckham, S.H., Avens, L., y Kurle, C.M., 2017a. Intrapopulation variability in the timing of ontogenetic habitat shifts in sea turtles revealed using δ15N values from bone growth rings. J. Anim. Ecol. 86 (3), 694–704. https://doi.org/10.1111/1365-2656.12618.

Turner Tomaszewicz, C.N., Seminoff, J.A., Price, M., Kurle, C.M., 2017b. Stable isotope discrimination factors and between-tissue isotope comparisons for bone and skin from captive and wild green sea turtles (Chelonia mydas). Rapid Commun. Mass Spectrom. 31 (22), 1903–1914. https://doi.org/10.1002/rcm.7974.

Varo-Cruz, N., Bermejo, J.A., Calabuig, P., Cejudo, D., Godley, B.J., López-Jurado, L.F., Pikesley, S.K., Witt, M.J., y Hawkes, L.A., 2016. New findings about the spatial and temporal use of the Eastern Atlantic Ocean by large juvenile loggerhead turtles. Divers. Distrib. 22 (4), 481–492. https://doi.org/10.1111/ddi.12413.

Wallace, B.P., Posnik, Z.A., Hurley, B.J., DiMatteo, A.D., Bandimere, A., Rodriguez, I., Maxwell, S.M., Meyer, L., Brenner, H., Jensen, M.P., LaCasella, E., 2023. Marine turtle regional management units 2.0: an updated framework for conservation and research of wide-ranging megafauna species. Endanger. Species Res. 52, 209–223. https://doi.org/10.3354/esr01243.

Yoshida, N., Miyazaki, N., 1991. Oxygen isotope correlation of cetacean bone phosphate with environmental water. J. Geophys. Res.: Oceans 96 (C1), 815–820. https://doi.org/10.1029/90JC01580.

Zug, G.R., Wynn, A.H., Ruckdeschel, C., 1986. Age determination of loggerhead sea turtles, *Caretta caretta*, by incremental growth marks in the skeleton. In: Smithsonian Contributions to Zoology, vol. 427. Smithsonian Institution Press, City of Washington, pp. 1–34.